

# Content-adaptive Representation Learning for Fast Image Super-resolution

Yukai Shi <sup>\*</sup>, Jinhui Qin <sup>\*</sup>

arXiv:2105.09645v1 [cs.CV] 20 May 2021

**Abstract**—Deep convolutional networks have attracted great attention in image restoration and enhancement. Generally, restoration quality has been improved by building more and more convolutional block. However, these methods mostly learn a specific model to handle all images and ignore difficulty diversity. In other words, an area in the image with high frequency tend to lose more information during compressing while an area with low frequency tends to lose less. In this article, we address the efficiency issue in image SR by incorporating a patch-wise rolling network(PRN) to content-adaptively recover images according to difficulty levels. In contrast to existing studies that ignore difficulty diversity, we adopt different stage of a neural network to perform image restoration. In addition, we propose a rolling strategy that utilizes the parameters of each stage more flexible. Extensive experiments demonstrate that our model not only shows a significant acceleration but also maintain state-of-the-art performance.

**Index Terms**—Image Super Resolution, Convolution Neural Network, Acceleration

## I. INTRODUCTION

Deep learning has successfully applied in many computer vision fields such as image recognition [16], semantic segmentation [30] and object detection [26]. Inspired by the rapid development and superior performance, many efforts have been made to introduce deep learning in low-level vision as well as image processing tasks, including image super-resolution [5], image enhancement [15], inpainting [29] etc. Meanwhile, Single image super-resolution(SISR), namely to predict high-resolution with low-resolution input, is widely used in many computer vision applications and draws plenty of attentions [4], [5], [18], [19], [22], [24], [34].

Recently, Convolutional neural networks(CNNs) achieve magnificent improvement toward image restoration by adopting a building block strategy. VDSR [18] utilizes residual connection and a very deep model to achieve promising results in image SR. EDSR [24] further improves the results by adopting residual block [16] and remove batch normalization. However, they advance performance with numerous parameter gain and huge computational cost. Dense block [12] also exhibits its effectiveness in image enhancement. MemNet [37] realizes a coarse-to-fine restoration process by using dense block and recursive unit. Zhang *et al.* [45] proposes an optimized block, which combines the strengths of the dense block and residual block, and achieve impressive promotion. However, deep learning-based SR methods [18], [24], [37], [45] prefer to crop the image into patches before training

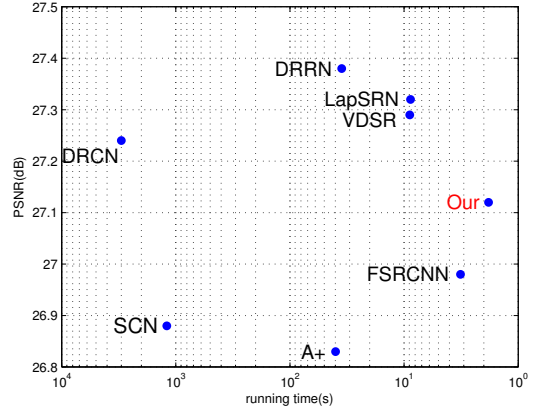


Fig. 1: Efficiency analysis of the proposed model. The results are evaluated on BSDS100 with factor 4×. The proposed model runs twice as fast as state-of-the-art SR inferences with superior performance.

phrase. As different patch has various texture and structure, it is inefficient to adopt a feed-forward network to super-resolve all samples, especially for those *intensely simple* patches. In addition, notwithstanding such a complicated model can bring positive performance with a graphics processing unit(GPU), it also leads to expensive computational cost and explosion of parameters.

Computer vision applications and technongies [10], [15], [44] for mobile devices draw a lot of attention as it has wide application scenarios. However, using CNNs on the mobile platform has an extreme requirement towards efficiency. MobileNet [10] makes an attempt to accelerate speed by utilizing a depth-wise convolution to reduce redundancy of CNNs. Similar technology also adopted by ShuffleNet [44]. Moreover, ShuffleNet employs a novel shuffle unit, which maintains performance with efficiency improvement. However, their methods are limited by the optimization of the computational platform and sometimes run inefficiently. IGC [43] utilizes parameters of the deep network more efficiently by adopting group convolution and permutation of convolutional features. The similar idea also used by RRC [28]. RRC implements a rolling strategy on object detection, which not only utilizes multi-scale features but also realizes an efficient one-stage framework. Their methods reveal that features of different scale can be utilized more efficiently. MSDNet [11] proposes a multi-scale dense net, which adaptively uses the specific stage in the deep model to deal with samples with

<sup>\*</sup> The first two authors share first-authorship.

different difficulty levels. For instance, MSDNet adopts early stage convolutional layers to handle easy samples and more parameters are applied to process difficult images. However, MSDNet can inherently distinguish difficult level with an internal high-level representation of the image itself. Since such internal high-level prior is not exist in low-level vision, MSDNet is fail to applied in images processing tasks.

Motivated by previous works, we make an attempt to propose a content-adaptive and flexible framework, which can accurately super-resolve image with different difficulty level according to gradient prior. In the proposed model, we first define the gradient prior to distinguish different samples. Then, a unified model is proposed to handle samples with different difficulty by a content-adaptive fashion. Since samples with different difficulty will cause frequency conflicts and result in a performance degradation. We also propose a flexible rolling strategy by alternating the convolution filters to address this problem.

Our main **contributions** are summarized as follows.

- We find it is inefficient to adopt an expensive model to mild samples, which have less texture and simple structure. In contrast, an expensive model is appropriate for the samples, which have rich texture and complicated structure.
- According above observation, we distinguish the difficulty of samples by its gradient prior and content-adaptively adopt different convolutional stage to super-resolve samples. This strategy helps us greatly improve SR efficiency.
- Since the samples with different difficulty exhibit various property in the frequency domain, which causes frequency conflicts and leads to a performance degradation. We propose a flexible rolling strategy. With our rolling approach, our model not only achieve a balance between mild and severe samples but also increase the receptive field of early layers.

## II. RELATED WORK

**CNN for image SR.** Recently, deep learning based SR methods have achieved a great successes in many computer vision fields. Super-resolution, which considered a typical low-level vision task and is well-known for its ill-posed property, plays an important role in image quality enhancement. Many researchers devote themselves to the studies of super-resolution and have proposed many insightful works. Recently, the rising of deep learning methods give new solution to image SR. Dong *et al.* [5] first adopt deep convolutional neural networks to learn the mapping from LR to HR patches in an end-to-end manner and greatly boost the performance of image SR. Afterward, many deep learning based methods have been proposed to improve the performance mainly by developing the network architecture. VDSR [18] and IRCNN [42] increased the network depth by adding more convolutional layers, and DRCN [17] introduced recursive learning for parameter sharing. Tai *et al.* introduced recursive blocks in DRRN [36] and memory block in Memnet [37]. While all of these methods have greatly improved the SR performance

by exploiting different network architecture, they have not considered the efficiency of SR, which lead to the learning based SR methods been away from application in reality.

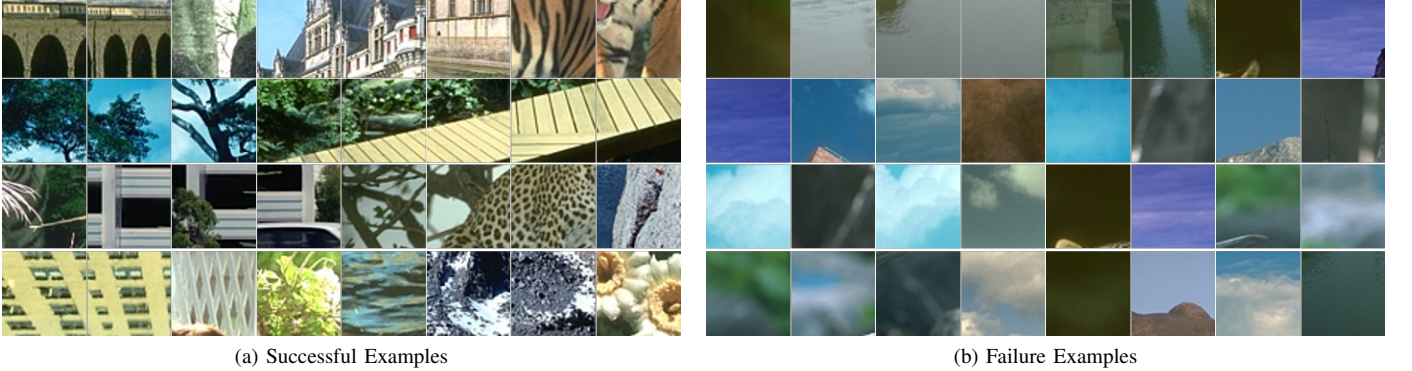
In contrast to chasing a smaller mean square error, we focus on the improvement of image restoration quality as well as boost the speed of the algorithm, which has been neglected for a long time. FSRCNN [4] make an attempt to address this issue by adopting down-sampled patches as input and deconvolution to speed up the computing process. Their method effectively reduce redundancy and inspired us to explore the potential of accelerating SR. ESPCN [35] used pixel shuffling operation to reduce features volume and checkerboard effect, which also greatly accelerated the SR network. Although these methods obtain a small running time, they don't fully utilize the inherent property of SR problem. For image SR, it has internal difficulty diversity, that is an area of an image with high frequency tend to lose more information during compressing while an area with low frequency tends to lose less. However, aforementioned methods ignore this property and tend to adopt a feed-forward model to process all samples.

**Neural network acceleration.** Obtaining a better balance between accuracy and efficiency has attracted many research communities for decades. Many studies have been proposed to change the connectivity structure of the deep convolutional networks such as ShuffleNet [44] or introduce a more compact convolution operation such as in MobileNet [10] and MobileNetV2 [31]. These studies have done great in reducing computation cost as well as maintain or even improve performance. However, these methods can be slower than a plain network in some computing platform. Some studies focus on reducing model size after training, such as weight pruning [21], [23], weight quantization [14], [27]. These studies construct new models at the test time and re-train or fine-tune them to achieve a similar closer performance as the original models.

Other studies focus on alternating the evaluation manner. FractalNets [20] perform prediction at any time by progressively evaluating subnetworks of the full network. Bolukbasi *et al.* [2] addresses this problem by adaptively evaluating neural networks. Different from these works, MSDNet [11] adopts a specially designed network with multiple classifiers, which can directly output confidence scores to control the evaluation process for each test example. The adaptive computation time method [9] and its extension [7] also perform an adaptive evaluation of test examples but focus on skipping units rather than layers. Feedback Networks [41] heavily shares parameters and allows early predictions in a recurrent process. However, their methods are less efficient in sharing computation. Our method is most inspired by MSDNet. Different from MSDNet, our proposed method focus on the difficulty diversity of image itself. And we also explore the frequency conflict occurred in a single model and therefore propose an original rolling strategy to handle the conflict.

## III. METHODOLOGY

**Problem.** We investigate the failure cases which lead to poor performance in image SR. Given a 7-layers CNN, which



(a) Successful Examples

(b) Failure Examples

Fig. 2: Visualization results of a regular CNN for image SR. Left examples bring enormous PSNR(dB) promotion towards Bicubic. Right samples have higher absolute PSNR(dB) value as they contribute slight PSNR(dB) gain compared with Bicubic. It reveals that CNN is feasible to restore abundant texture images and bring great promotion, as patches with mild texture own a tiny upper bound.

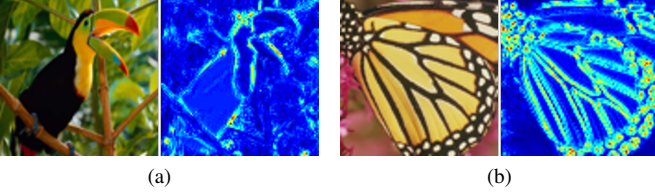


Fig. 3: The features of *bird* and *butterfly* are visualized in (a) and (b). For better visualization, we reduce dimension to 1 along channel with max operation.

has 6 convolutional layer with size of  $3 \times 3 \times 32$  and a convolutional layer with size of  $3 \times 3 \times 1$ , we train it with 10 epochs on General-100 [4] to super-resolve images with factor  $\times 3$ , we test it on BSDS100 [1]. In Figure.2b and 2a, we visualize its successful and failure examples. Meanwhile, we define the examples, which achieve more than 1dB improvement over Bicubic, as successful cases. The failure cases are the smaller images that obtain improvement less than 1dB. In Figure.2b, we can observe that the examples, which achieve minor improvement, are mild or inherently blurry. In contrast, the successful cases have a rich texture and drastic gradient. Moreover, we also extract feature in the middle of VDSR [18] and present it in Fig. 3a and 3b. It can be observed that responses around high-frequency places are strong and VDSR gives low response toward the mild place.

According to our observation, we make three assumptions as follow. 1) The examples with rich texture can bring enormous gain. However, the mild examples are unable to demonstrate similar improvement. 2) Since deep neural network gives low response toward mild places and mild examples is intensely simple. A very deep neural network, which is widely used in image SR, owns a slight contribution to mild samples for further promotion. 3) The examples with severe, moderate and mild texture can be easily distinguished with its gradient information. To address the aforementioned problems, we propose an end-to-end framework that joint learning image

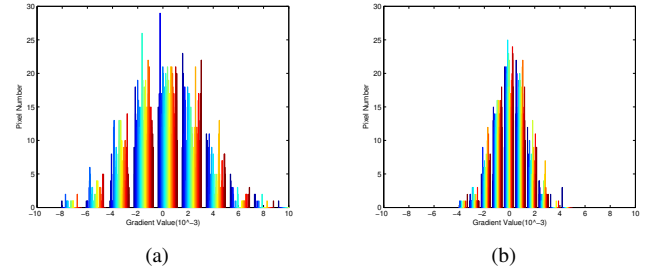


Fig. 4: Gradient properties of 10,000 severe and mild images. (a) Distribution of vertical axis gradient from high PSNR(dB) gain samples(e.g., severe images) in Figure.2a. (b) Distribution of vertical axis gradient from small PSNR(dB) gain cases(e.g., mild images) in Figure. 2b. We can easily distinguish successful and failure samples according to the gradient value.

SR task with gradient prior knowledge.

**Overview of PRN.** The proposed PRN aims at learning a framework, which can super-resolve images more efficiently. More specific, the proposed framework first label patches according to gradient prior. Thus, we can fetch the different patches from different feature level. Since the bottom convolutional stage has tiny receptive field and the mild patches is different from severe samples in term of frequency, we then relieve these problems by adopting a novel strategy to roll convolutional filters. Next, we first describe the definition of gradient prior and then present the setting of the proposed framework.

#### A. Gradient Prior

The proposed gradient prior is based on the observations that the failure samples in image SR usually have uniform gradient without sharp edges. As the samples with a uniform gradient contain rare pattern information and the upper bound for restoration is also pretty low, a simple and fast convolutional neural network can handle them well. We show the

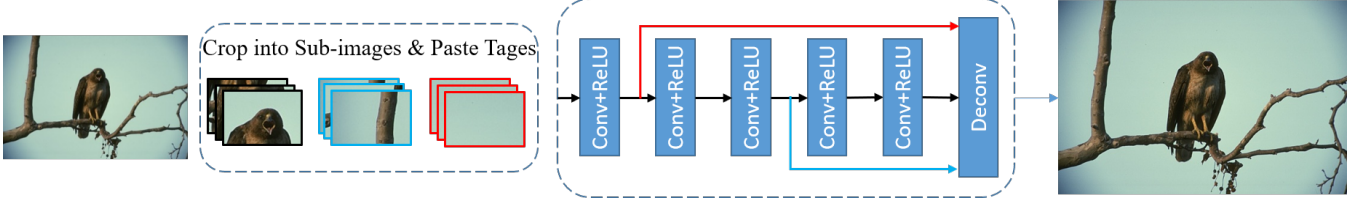


Fig. 5: Overview of the proposed PRN. The input image has plenty of blank regions and therefore we fetch results from the different position within the network to boost efficiency. We use **red**, **blue** and **black** bbox to label mild, moderate and severe patches and then send them into the network. The sub-images with different gradient prior will be fetched from the different convolutional layer. The arrow lines with the corresponding color indicate the stage where we fetch different patches. With this strategy, our method demonstrates a significant efficiency improvement.

vertical gradient distribution of 10,000 successful and failure samples in Figure 4a and 4b, respectively. It is obvious that mild samples have denser distribution among lower vertical gradient. And the distribution of severe images mainly lies on large value. With this gradient property, severe and mild samples can be distinguished. For an image, we describe the gradient property as follow:

$$P(x) = \|G_{ver}(x)\|, \quad (1)$$

where  $x$  is the input image,  $G_{ver}$  counts the gradient along the vertical axis.  $P$  are the gradient prior knowledge, which also serves as a tag in our model. With the  $P$ , PRN is able to separate a set of images into mild, moderate and severe patches.

$$\begin{cases} \text{Mild} & P \leq \gamma_{upper} \\ \text{Moderate} & \gamma_{upper} \leq P \leq \gamma_{low} \\ \text{Severe} & \gamma_{low} \leq P. \end{cases} \quad (2)$$

The  $\gamma_{upper}$  and  $\gamma_{low}$  means the upper and low gradient threshold of  $P$  for separating the images. Moreover, we make an ablation study on the gradient threshold in section IV-B. Although  $P(x)$  is proposed based on the assumption that mild texture image is too simple to bring enormous gain, we show this prior can also be applied to accelerate image SR.

## B. Network architecture

As illustrated in Fig.5, we put the patches with tag into the network for enhancement. To enable the network with a spacious receptive field, we use 64 convolutional kernels with a size of  $5 \times 5$ . To make full use of cuDNN [3], we employ 4 convolutional layers with  $3 \times 3$  kernels and 64 channels. Before deconvolution operation, we conduct a shrinking layer with 64 kernels of size  $1 \times 1$  to reduce parameters. Meanwhile, we add Leaky ReLU [25] as activation function after each convolutional layer. Due to the efficient  $3 \times 3$  kernels work on small size feature map directly, the proposed model can significantly accelerate the speed. At last, we use a deconvolution layer, whose stride is same to down-sampling factor, to perform an up-sampling operation.

To obtain higher efficiency, we join auxiliary tag into our model by an end-to-end manner. In other words, the patch is able to be fetched from different feature level w.r.t tag

knowledge. Since the mild patches are smooth and have less edge and texture, we prefer to obtain its feature from the first convolutional layer. Then, we use a deconvolution layer to obtain the restored patches. For moderate samples, we fetch from the third convolutional layer as they have a few texture and edge. A similar up-sampling operation also acts on the moderate samples for interpolation. Due to severe patches have rich texture and details, we conduct deconvolution layer on them after they forward all convolutional layers. The parameter of the network is optimized by  $L_2$  loss. Meanwhile, different level of parameters is learned with different training pairs. For instance, the early stage layer is not only training with mild image pairs but also optimized with severe pairs. In contrast, the high-level parameter is optimized with severe pairs only. As shown in Fig.5, we adopt such an efficient strategy to perform image SR.

## C. Rolling the convolutional filters

Although we can effectively enhance the image with the aforementioned model, we still find the following problems: 1) The receptive field of the early stage is tiny. When we try to improve the performance, the tiny receptive field of early stage become a bottleneck. 2) Frequency conflicts. The frequency domain of mild and moderate examples are significantly different from severe patches. When we train mild samples in the early stage of the network, the output of high level is influenced. Thus, we make an attempt to resolve the above questions by developing a novel rolling strategy.

Let  $\Theta$  be parameters of a CNN, it consists of four parts of parameters  $\{\Theta_l, \Theta_m, \Theta_s, \Theta_{up}\}$ . Meanwhile,  $\Theta_l$  represents the early stage and consists of a convolutional layer.  $\Theta_m$  means the middle stage and has two layers.  $\Theta_s$  indicates the last stage and contains two convolutional layers and  $\Theta_{up}$  is the parameters of a deconvolutional layer. In addition, we define auxiliary two set of the parameter  $\Theta_l^D$  and  $\Theta_m^D$ . More specific,  $\Theta_l^D$  represent a dilated convolution layer [40] with size of  $64 \times 5 \times 5$  and 1 dilation and  $\Theta_m^D$  means two dilated convolution layers with size of  $64 \times 3 \times 3$  and 1 dilation as well. We use  $\mathbb{P}_{HR}$  and  $\mathbb{P}_{LR}$  represent high-res and low-res patch, respectively. Three superscripts  $l$ ,  $m$  and  $s$  are utilized to distinguish the mild, moderate and severe samples respectively. For instance,  $\mathbb{P}_{LR}^l$  and  $\mathbb{P}_{LR}^s$  indicate the low-res patch annotated with mild and

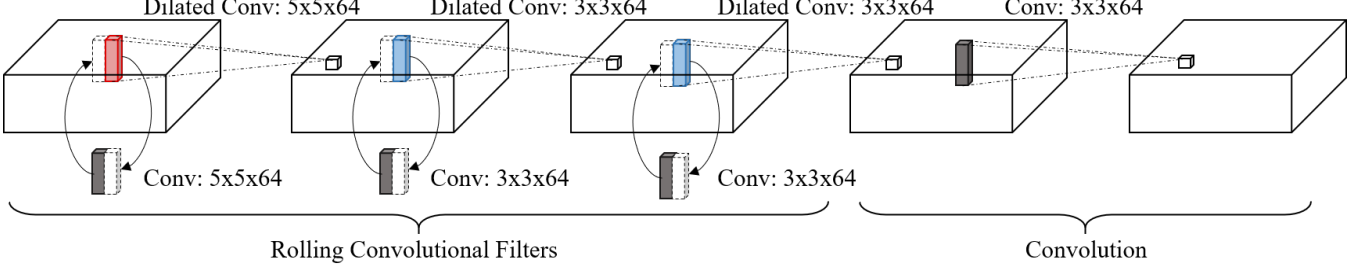


Fig. 6: Demonstration of the rolling strategy. The parameters for different patches(e.g., mild, moderate and severe) are label with **red**, **blue** and **black**. When we input the severe patch, the model roll the first three dilated convolutional layers(e.g., **red** and **blue** columns) with regular convolutional layers(e.g., **black** column). Nevertheless, suppose we send mild patch into the model, the model will replace dilated convolution(e.g., **red**) with regular convolution layer(e.g., **black** column). With this content-adaptive and flexible strategy, our model improve the effectiveness and efficiency significantly.

severe tag. In sum, the enhancement toward severe patch can be defined as:

$$\mathbb{P}_{out} = f(\mathbb{P}_{LR}^s | \Theta_l, \Theta_m, \Theta_s, \Theta_{up}), \quad (3)$$

where  $f$  means the enhancement operation. As sketched in Fig. 6, the network will roll  $\Theta_l$  and  $\Theta_m$  with  $\Theta_l^D$  and  $\Theta_m^D$  and fetch the patch from different stage according to tag. More specific, suppose we input  $\mathbb{P}_{LR}^l$  into the network, the model will enhance the patch with  $\Theta_l^D$  explicit. By that analogy, the enhancement process toward  $\mathbb{P}_{LR}^l$  and  $\mathbb{P}_{LR}^m$  can be formulated as

$$\mathbb{P}_{out} = f(\mathbb{P}_{LR}^l | \Theta_l^D, \Theta_{up}) \quad (4)$$

and

$$\mathbb{P}_{out} = f(\mathbb{P}_{LR}^m | \Theta_m^D, \Theta_{up}). \quad (5)$$

With such flexible and content-adaptive rolling strategy, we not only resolve frequency conflicts but also increase the receptive field of early stage.

#### D. End-to-end framework

In contrast to training models with different datasets, the proposed model not only be able to fetch images from the different stage but also optimize each stage with specific prior. The whole procedure can be formulated as an end-to-end framework to accelerate speed. We have sketch detailed algorithm in Algorithm.1. Since the down-scaled mild sample is similar to its ground-truth, the model is unable to learn how to recover realistic details and textures w.r.t mild training examples. To resolve this question, we adopt the mild and moderate samples as the training pairs for  $\Theta_l^D$  and  $\Theta_m^D$ . With such an efficient strategy, our model not only greatly improve the performance but also accelerate the training and testing speed.

## IV. EXPERIMENTS

**Datasets.** To make full use of the parameters in PRN, we use VOC2012 [6] to pre-train our model. VOC2012 [6] contains 17,125 clear images, which are taken from natural scene. Then, we finetune our model with BSD200 [1], which contains 200 images and is close to the real-world scene.

---

#### Algorithm 1 Learning Algorithm of PRN

---

**Require:** Training LR images  $I_{LR}$ ; HR images  $I_{HR}$ ;

- 1: Crop high-res and low-res images into patches  $\mathbb{P}_{LR}$  and  $\mathbb{P}_{HR}$  and distinguish  $\mathbb{P}_{LR}$  into  $\mathbb{P}_{LR}^l$ ,  $\mathbb{P}_{LR}^m$  and  $\mathbb{P}_{LR}^s$  w.r.t gradient prior;
- 2: **while**  $t < T$  **do**
- 3:    $t \leftarrow t + 1$ ;
- 4:   Choose a set of LR and HR patches, send low-res patches into network;
- 5:   Obtain  $f(\mathbb{P}_{LR}^m | \Theta_l^D, \Theta_m^D, \Theta_{up})$ ,  $f(\mathbb{P}_{LR}^l | \Theta_l^D, \Theta_{up})$   $f(\mathbb{P}_{LR}^s | \Theta_l, \Theta_m, \Theta_s, \Theta_{up})$  via forward propagation;
- 6:   Update  $\{\Theta_l^D, \Theta_{up}\}$  with  $\mathbb{P}_{LR}^l$  and  $\mathbb{P}_{HR}$  pairs;
- 7:   Update  $\{\Theta_m^D, \Theta_{up}\}$  with  $\mathbb{P}_{LR}^m$  and  $\mathbb{P}_{HR}$  pairs;
- 8:   Update  $\{\Theta_l, \Theta_m, \Theta_s, \Theta_{up}\}$  with  $\mathbb{P}_{LR}^s$  and  $\mathbb{P}_{HR}$  pairs;
- 9: **end while**

---

BSD200 [1] is augmented with scaling and rotation. We employ Set5, Set14, BSDS100, and Urban100 to evaluate our model.

**Implementation Details.** We use Xavier [8] initialize the parameters of the proposed model. Besides, the deconvolution layer is initialized according to the weight of Bicubic interpolation. We add pad with zero in each convolutional layer to assure the input tensor shares same size with the output. We convert all images from RGB to YCbCr and extract the Y channel for training. The training and testing images are cropped into  $54 \times 54$  patches and down-scaled with the corresponding factor to obtain the input. For  $54 \times 54$  patch, the  $\gamma_{upper}$  and  $\gamma_{low}$  are set as  $1 \times 10^1$  and  $3 \times 10^1$ , respectively. In training, we set the batch size as 64 and learning rate is  $1 \times 10^{-4}$  for all layers. In testing, we set the batch size as 1. The learning rate is reduced with factor  $\times 10$  for every 300 epochs. We use leaky ReLU with a negative slope of 0.2 as the activate function. We perform our training and testing on a desktop computer with i7-4790 CPU, GTX980Ti GPU, and 32GB RAM.

**Multi-scale training.** Different from some state-of-the-arts [4], [5], [34], which conduct its model with single factor training, we adopt multi-scale learning strategy to train PRN. Specifically, multi-scaling learning is to train the

model with multiple down-sampling factors simultaneously. With the multi-scale learning, PRN can learn more contextual knowledge across different degeneration and achieves better performance.

### A. Comparison with State-of-the-arts.

We compare our model with state-of-the-art methods, including A+ [38], SRF [32], SelfEx [13], RFL [33], SCN [39], SRCNN [5], LapSRN [19], VDSR [18], DRCN [17], and FSRCNN [4]. We adopt widely used quality metrics, e.g., PSNR and SSIM, to evaluate our model. For DRCN [17], we use our own implementation for comparison. For rest of other methods, we use their public code and model to obtain results.

As shown in table. I, our model achieve superior performance among light-weight methods [4], [5], [13], [32], [33], [38], [39]. Compared with FSRCNN, our model achieve 0.13 dB and 0.19 dB promotion on BSDS100 with factor 2 $\times$  and 3 $\times$ . Similarly, our model obtains 0.69 dB gain when compared with FSRCNN on Mange109 with factor 4 $\times$ . With the limitation of the parameter, our model is weak than heavy inferences [17]–[19]. As sketched in figure. 1, our model shows slightly lower performance compared with huge model [17]–[19], but our speed is accelerated about several times. Therefore, the model is particularly competitive for mobile devices and applications.

We also show qualitative comparison in Figure. 8, 9, 10 and 11. For better visualization, we interpolate the chrominance space by bicubic to obtain color images. Compared with other methods, our approach can generate image clearer boundary and rich details.

### B. Ablation study

In this section, we mainly investigate different settings of the proposed model and provide insights into the choice of hyper-parameters.

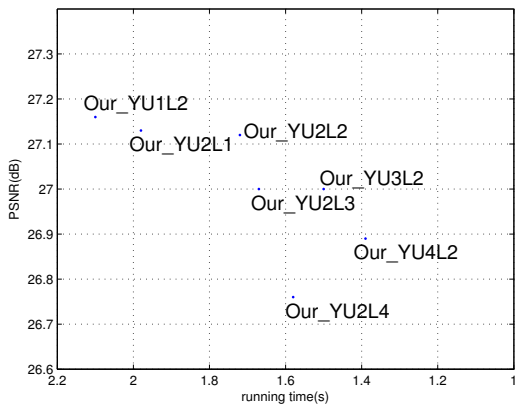


Fig. 7: Efficiency and effectiveness analysis of different gradient threshold on BSDS100.

**Gradient threshold.** We first analyze the setting of gradient threshold  $\gamma_{upper}$  and  $\gamma_{low}$  by investigating a wide range of

potential values. In table II, we list all threshold we have compared. In fact, different gradient threshold may influence efficiency and effectiveness. In Fig. 7, we show the performance and efficiency of each setting. With the increment of  $\gamma_{low}$ , our model deal more moderate samples at an early stage, which accelerate speed but bring significant performance drop. A similar situation also occur when we increase the value of  $\gamma_{upper}$ . As the growth of  $\gamma_{upper}$ , the proposed model exhibit promising efficiency with degradation of performance. Since the middle or first stage is unable to deal severe samples well, we think too low  $\gamma_{upper}$  and  $\gamma_{low}$  may bring obvious performance drop. However, as illustrated in Fig. 7, the model becomes slower with a decrease of  $\gamma$ . To achieve a balance between efficiency and performance, we adopt ‘Our\_YU2L2’ as default gradient threshold.

**Depth of different stage.** In this component, we compare the depth setting of each stage. In other words, we adjust the depth of  $\Theta_l$  and  $\Theta_m$  to verify our settings. In table. III, we use different depth setting in the early and middle stage for comparison. As shown in table. III, with the increase of  $\Theta_l$ , the model show slight PSNR promotion with slower efficiency. Since the early stage is adapted to handle mild patches only, we think too much parameter is meaningless for further promotion. In contrast, the middle stage  $\Theta_m$  is utilized to deal with the moderate sample, which carries some texture and details. Therefore, the performance becomes worse when we reduce parameter of  $\Theta_m$ . Thus, we use a light-weight setting at an early stage and increase the parameters of the middle stage to exhibit an efficient framework.

**Rolling strategy.** In order to show the effectiveness of the proposed rolling strategy, we investigate models with and without rolling strategy. In table. IV, ‘o Rolling’ means model without rolling strategy and ‘Rolling’ indicates the model with rolling component. Compared with ‘o Rolling’, the model with a rolling strategy achieve 0.09 dB improvement. Although our model has an auxiliary parameter, we can use them content-adaptively to assure efficiency. Thus, our model achieves superior performance and maintains competitive efficiency by adopting a rolling strategy.

### C. Limitations

As our model achieves a good balance between effectiveness and efficiency, it still exists some limitations. To advance efficiency, we need to crop the image into smaller images and reconstruct them at last. Thus, our model needs additional time to accomplish the reconstruction procedure. The reconstruction cost is far less than the model computational cost, and we have count the reconstruction time into time complexity in efficiency analysis. Besides, the acceleration is influenced by datasets. For instance, our model can accelerate the speed greatly on BSDS100 or DIV2K as the images in BSDS100 or DIV2K have plenty of blank and mild region. Similar acceleration can not occur in General-100 as the images in General-100 are full with texture and edges. However, we think the majority of nature images, which is closed to BSD500 and DIV2K, are occupied with a certain percentage of the blank or mild region. Therefore, our model can perform similar acceleration in real-world scenarios.

Algorithm	Scale	Set5		Set14		BSDS100		URBAN100	
		PSNR	SSIM	PSNR	SSIM	PSNR	SSIM	PSNR	SSIM
Bicubic	2x	33.69	0.931	30.25	0.870	29.57	0.844	26.89	0.841
		36.60	0.955	32.32	0.906	31.24	0.887	29.25	0.895
		36.59	0.954	32.29	0.905	31.18	0.885	29.14	0.891
		36.60	0.955	32.24	0.904	31.20	0.887	29.55	0.898
		36.72	0.955	32.51	0.908	31.38	0.889	29.53	0.896
		36.58	0.954	32.35	0.905	31.26	0.885	29.52	0.897
		37.05	0.956	32.66	0.909	31.53	0.892	29.88	0.902
SRCNN	3x	<b>37.09</b>	<b>0.957</b>	<b>32.90</b>	<b>0.910</b>	<b>31.66</b>	<b>0.893</b>	<b>30.23</b>	<b>0.909</b>
		30.41	0.869	27.55	0.775	27.22	0.741	24.47	0.737
		32.62	0.909	29.15	0.820	28.31	0.785	26.05	0.799
		32.47	0.906	29.07	0.818	28.23	0.782	25.88	0.792
		32.66	0.910	29.18	0.821	28.30	0.786	26.45	0.810
		32.78	0.909	29.32	0.823	28.42	0.788	26.25	0.801
		32.62	0.908	29.16	0.818	28.33	0.783	26.21	0.801
FSRCNN	4x	33.18	0.914	29.37	0.824	28.53	0.791	26.43	0.808
		<b>33.32</b>	<b>0.916</b>	<b>29.64</b>	<b>0.828</b>	<b>28.72</b>	<b>0.794</b>	<b>26.75</b>	<b>0.815</b>
		28.43	0.811	26.01	0.704	25.97	0.670	23.15	0.660
		30.32	0.860	27.34	0.751	26.83	0.711	24.34	0.721
		30.17	0.855	27.24	0.747	26.76	0.708	24.20	0.712
		30.34	0.862	27.41	0.753	26.84	0.713	24.83	0.740
		30.50	0.863	27.52	0.753	26.91	0.712	24.53	0.725
SCN	4x	30.41	0.863	27.39	0.751	26.88	0.711	24.52	0.726
		30.72	0.866	27.61	0.755	26.98	0.715	24.62	0.728
		<b>31.08</b>	<b>0.875</b>	<b>27.89</b>	<b>0.762</b>	<b>27.17</b>	<b>0.728</b>	<b>24.86</b>	<b>0.733</b>

TABLE I: The PSNR and SSIM results of different approaches on Set5, Set14, BSDS100 and Urban100 with down-sampling factor  $\times 2$ ,  $\times 3$  and  $\times 4$ . We use the **black** to label the first place.

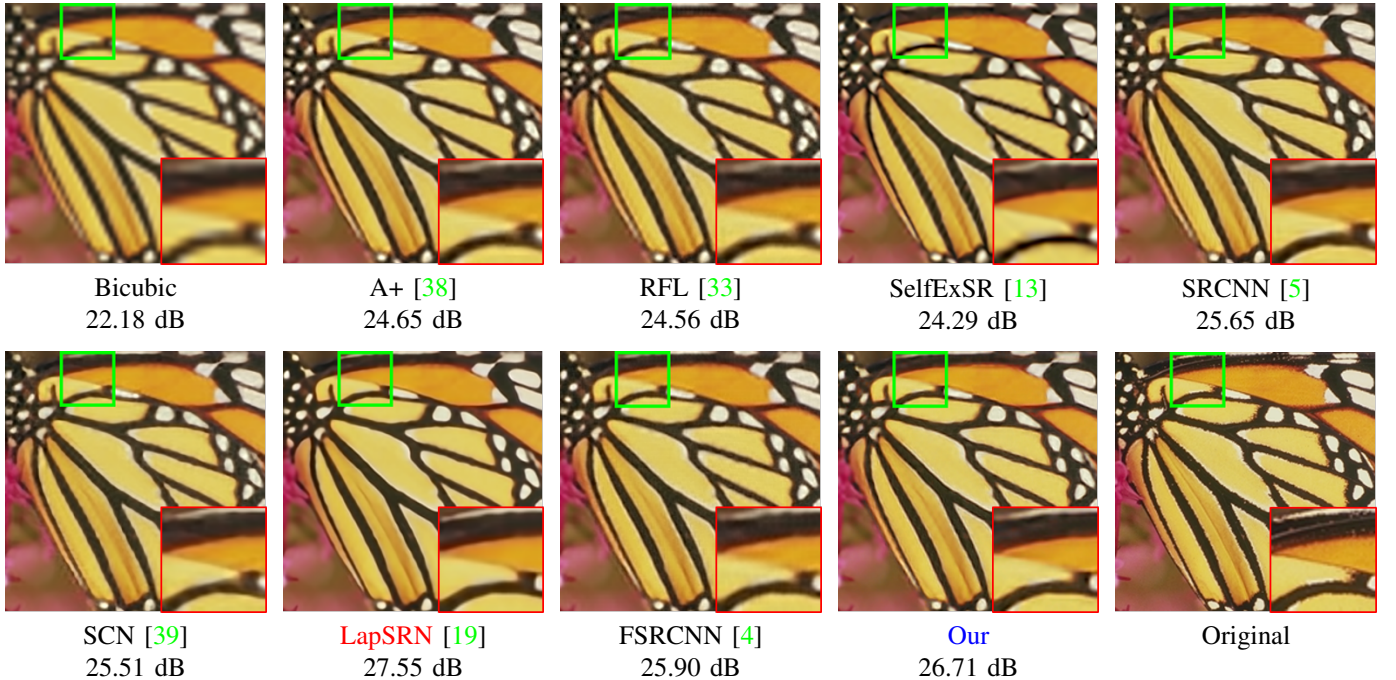


Fig. 8: Qualitative comparison on 'butterfly' with the scaling factor of 4. We use **red** and **blue** to label best two results, respectively. Best viewed by zooming in the electronic version.

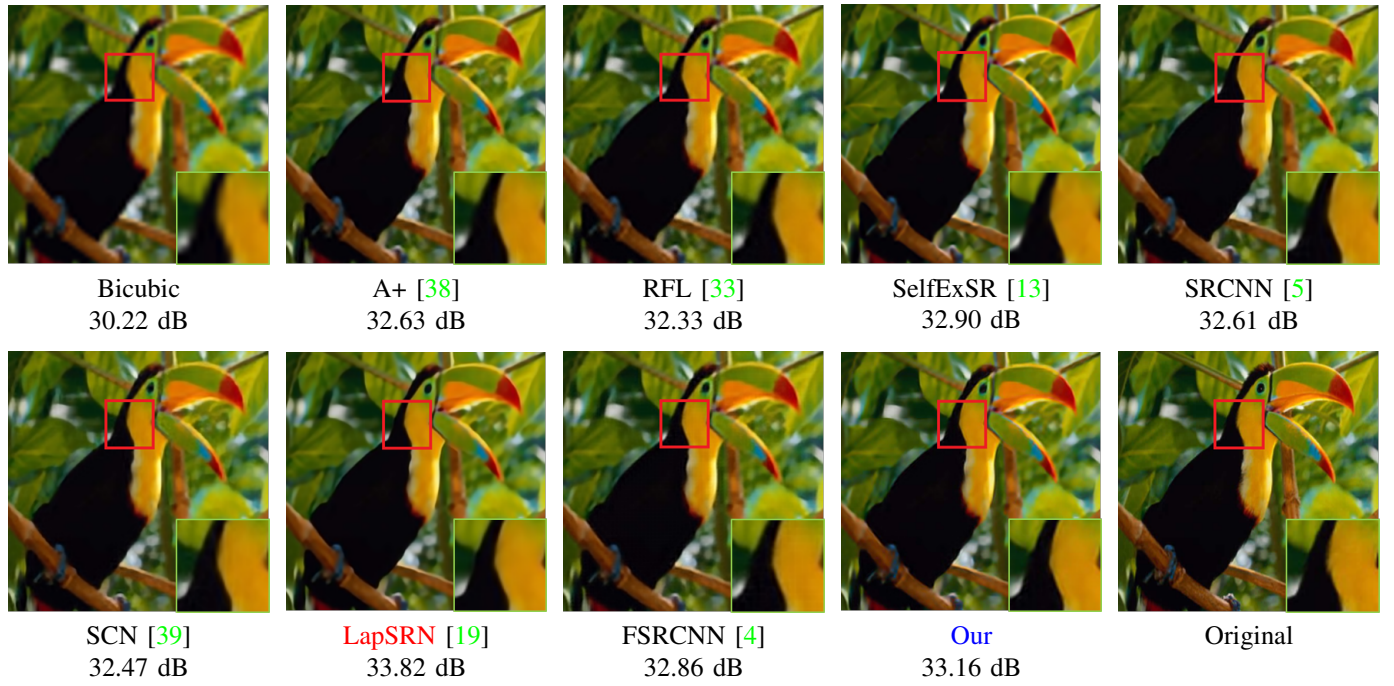


Fig. 9: Qualitative comparison on 'bird' with the scaling factor of 4. We use **red** and **blue** to label best two results, respectively. Best viewed by zooming in the electronic version.

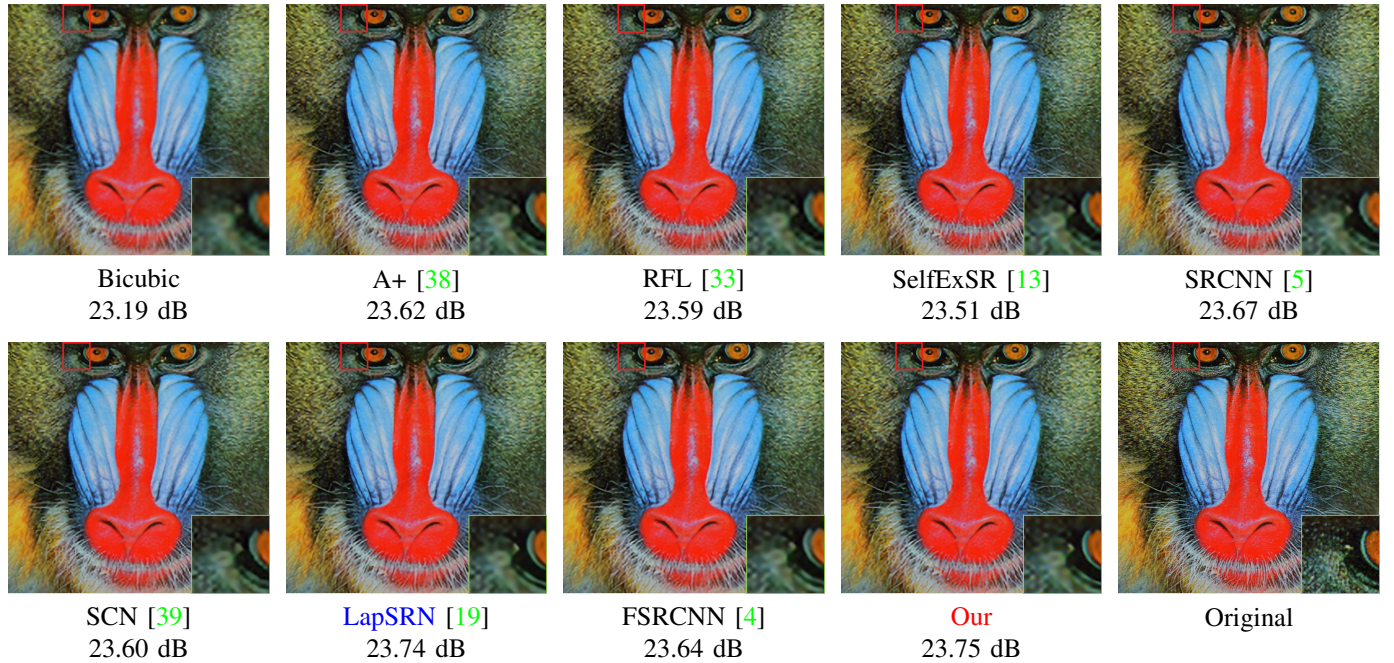


Fig. 10: Qualitative comparison on 'baboon' with the scaling factor of 3. We use **red** and **blue** to label best two results, respectively. Best viewed by zooming in the electronic version.



Fig. 11: Qualitative comparison on 'lena' with the scaling factor of 3. We use red and blue to label best two results, respectively. Best viewed by zooming in the electronic version.

$\gamma$	L1	L2	L3	L4	U1	U2	U3	U4
Value( $10 \times 1$ )	1	2	5	7	3	5	8	10

TABLE II: We have compared a wide range of potential gradient threshold. Meanwhile, L indicates  $\gamma_{low}$  and U is  $\gamma_{upper}$ . The suffix number along L and U means different threshold value.

	$\Theta_l^1$	$\Theta_l^2$	$\Theta_l^3$	$\Theta_m^1$	$\Theta_m^2$	$\Theta_m^3$
PSNR	27.12	27.13	27.15	27.05	27.12	27.15
Time	1.81	1.91	2.21	1.48	1.81	1.99

TABLE III: Comparison of different depth toward early and middle stage on BSDS100. The superscripts of  $\Theta$  mean different depth of each stage. The subscripts of  $\Theta$  indicate different stage.

## V. CONCLUSION AND FURTHER WORK

In this article, to address efficiency problem in image SR, we have proposed an end-to-end gradient-aware rolling network. Our model mainly incorporates gradient prior to the image itself and content-adaptively utilize each stage of the deep neural network to super-resolve corrupted images. Moreover, we have proposed a rolling strategy, which super-

	o Rolling	Rolling
PSNR	27.03	27.12

TABLE IV: Comparison of with and without rolling strategy on BSDS100.

resolve images with the different set of filters, to resolve frequency conflicts problem. Experiments have shown that our framework not only obtains competitive performance but also achieve appealing efficiency.

There are several directions for us to extend our work. First, we can introduce adversarial loss or perceptual loss in each stage, aiming to restore more realistic details and texture. Second, considering exist framework have to crop the image into patches, we intend to propose a more general framework, which can content-adaptively process different region with the different stride of convolution operation, to boost efficiency.

## REFERENCES

- [1] Pablo Arbelaez, Michael Maire, Charless Fowlkes, and Jitendra Malik. Contour detection and hierarchical image segmentation. *IEEE Trans. Pattern Anal. Mach. Intell.*, 33(5):898–916, May 2011.
- [2] Tolga Bolukbasi, Joseph Wang, Ofer Dekel, and Venkatesh Saligrama. Adaptive neural networks for fast test-time prediction. *CoRR*, *abs/1702.07811*, 2017.
- [3] Sharan Chetlur, Cliff Woolley, Philippe Vandermersch, Jonathan Cohen, John Tran, Bryan Catanzaro, and Evan Shelhamer. cudnn: Efficient primitives for deep learning. *Computer Science*, 2014.
- [4] Chao Dong, Changyuan Chen, and Xiaoxu Tang. Accelerating the super-resolution convolutional neural network. pages 391–407, 2016.
- [5] Chao Dong, Chen Change Loy, Kaiming He, and Xiaoxu Tang. Learning a deep convolutional network for image super-resolution. In *ECCV*, pages 184–199, 2014.
- [6] M. Everingham, L. Van Gool, C. K. I. Williams, J. Winn, and A. Zisserman. The PASCAL Visual Object Classes Challenge 2012 (VOC2012) Results.
- [7] Michael Figurnov, Maxwell D Collins, Yukun Zhu, Li Zhang, Jonathan Huang, Dmitry P Vetrov, and Ruslan Salakhutdinov. Spatially adaptive computation time for residual networks. In *CVPR*, volume 2, page 7, 2017.
- [8] Xavier Glorot and Yoshua Bengio. Understanding the difficulty of training deep feedforward neural networks. In *Proceedings of the thirteenth international conference on artificial intelligence and statistics*, pages 249–256, 2010.

[9] Alex Graves. Adaptive computation time for recurrent neural networks. *arXiv preprint arXiv:1603.08983*, 2016.

[10] Andrew G Howard, Menglong Zhu, Bo Chen, Dmitry Kalenichenko, Weijun Wang, Tobias Weyand, Marco Andreetto, and Hartwig Adam. Mobilenets: Efficient convolutional neural networks for mobile vision applications. 2017.

[11] Gao Huang, Danlu Chen, Tianhong Li, Felix Wu, Van Der Maaten Laurens, and Kilian Q Weinberger. Multi-scale dense networks for resource efficient image classification. 2017.

[12] Gao Huang, Zhuang Liu, Van Der Maaten Laurens, and Kilian Q Weinberger. Densely connected convolutional networks. pages 2261–2269, 2016.

[13] Jia Bin Huang, Abhishek Singh, and Narendra Ahuja. Single image super-resolution from transformed self-exemplars. In *Computer Vision and Pattern Recognition*, pages 5197–5206, 2015.

[14] Itay Hubara, Matthieu Courbariaux, Daniel Soudry, Ran El-Yaniv, and Yoshua Bengio. Binarized neural networks. In *Advances in neural information processing systems*, pages 4107–4115, 2016.

[15] Andrey Ignatov, Nikolay Kobyshev, Radu Timofte, Kenneth Vanhoey, and Luc Van Gool. Dslr-quality photos on mobile devices with deep convolutional networks. pages 3297–3305, 2017.

[16] Shaqiq Ren, Kaiming He, Xiangyu Zhang, and Jian Sun. Deep residual learning for image recognition. In *CVPR*. 2016.

[17] Jiwon Kim, Jung Kwon Lee, and Kyoung Mu Lee. Deeply-recursive convolutional network for image super-resolution. pages 1637–1645, 2015.

[18] Jiwon Kim, Jung Kwon Lee, and Kyoung Mu Lee. Accurate image super-resolution using very deep convolutional networks. 2016.

[19] Wei Sheng Lai, Jia Bin Huang, Narendra Ahuja, and Ming Hsuan Yang. Deep laplacian pyramid networks for fast and accurate super-resolution. 2017.

[20] Gustav Larsson, Michael Maire, and Gregory Shakhnarovich. Fractalnet: Ultra-deep neural networks without residuals. *arXiv preprint arXiv:1605.07648*, 2016.

[21] Yann LeCun, John S Denker, and Sara A Solla. Optimal brain damage. In *Advances in neural information processing systems*, pages 598–605, 1990.

[22] Christian Ledig, Zehan Wang, Wenzhe Shi, Lucas Theis, Ferenc Huszar, Jose Caballero, Andrew Cunningham, Alejandro Acosta, Andrew Aitken, and Alykhan Tejani. Photo-realistic single image super-resolution using a generative adversarial network. pages 105–114, 2016.

[23] Hao Li, Asim Kadav, Igor Durdanovic, Hanan Samet, and Hans Peter Graf. Pruning filters for efficient convnets. *arXiv preprint arXiv:1608.08710*, 2016.

[24] Bee Lim, Sanghyun Son, Heewon Kim, Seungjun Nah, and Kyoung Mu Lee. Enhanced deep residual networks for single image super-resolution. In *Computer Vision and Pattern Recognition Workshops*, pages 1132–1140, 2017.

[25] Andrew L. Maas, Awni Y. Hannun, and Andrew Y. Ng. Rectifier nonlinearities improve neural network acoustic models. In *in ICML Workshop on Deep Learning for Audio, Speech and Language Processing*, 2013.

[26] Wanli Ouyang, Xiaogang Wang, Xingyu Zeng, Shi Qiu, Ping Luo, Yonglong Tian, Hongsheng Li, Shuo Yang, Zhe Wang, Chen-Change Loy, et al. Deepid-net: Deformable deep convolutional neural networks for object detection. In *CVPR*, pages 2403–2412, 2015.

[27] Mohammad Rastegari, Vicente Ordonez, Joseph Redmon, and Ali Farhadi. Xnor-net: Imagenet classification using binary convolutional neural networks. In *European Conference on Computer Vision*, pages 525–542. Springer, 2016.

[28] Jimmy Ren, Xiaohao Chen, Jianbo Liu, Wenxiu Sun, Jiahao Pang, Qiong Yan, Yu Wing Tai, and Li Xu. Accurate single stage detector using recurrent rolling convolution. pages 752–760, 2017.

[29] Jimmy SJ Ren, Li Xu, Qiong Yan, and Wenxiu Sun. Shepard convolutional neural networks. In *NIPS*, pages 901–909, 2015.

[30] Olaf Ronneberger, Philipp Fischer, and Thomas Brox. *U-Net: Convolutional Networks for Biomedical Image Segmentation*. Springer International Publishing, 2015.

[31] Mark Sandler, Andrew Howard, Menglong Zhu, Andrey Zhmoginov, and Liang-Chieh Chen. Mobilenetv2: Inverted residuals and linear bottlenecks. In *Proceedings of the IEEE Conference on Computer Vision and Pattern Recognition*, pages 4510–4520, 2018.

[32] Samuel Schulter, Christian Leistner, and Horst Bischof. Fast and accurate image upscaling with super-resolution forests. In *Computer Vision and Pattern Recognition*, pages 3791–3799, 2015.

[33] Samuel Schulter, Christian Leistner, and Horst Bischof. Fast and accurate image upscaling with super-resolution forests. In *Computer Vision and Pattern Recognition*, pages 3791–3799, 2015.

[34] Wenzhe Shi, Jose Caballero, Ferenc Huszar, Johannes Totz, Andrew P. Aitken, Rob Bishop, Daniel Rueckert, and Zehan Wang. Real-time single image and video super-resolution using an efficient sub-pixel convolutional neural network. pages 1874–1883, 2016.

[35] Wenzhe Shi, Jose Caballero, Ferenc Huszár, Johannes Totz, Andrew P. Aitken, Rob Bishop, Daniel Rueckert, and Zehan Wang. Real-time single image and video super-resolution using an efficient sub-pixel convolutional neural network. In *Proceedings of the IEEE Conference on Computer Vision and Pattern Recognition*, pages 1874–1883, 2016.

[36] Ying Tai, Jian Yang, and Xiaoming Liu. Image super-resolution via deep recursive residual network.

[37] Ying Tai, Jian Yang, Xiaoming Liu, and Chunyan Xu. Memnet: A persistent memory network for image restoration. pages 4549–4557, 2017.

[38] Radu Timofte, Vincent De, and Luc Van Gool. Anchored neighborhood regression for fast example-based super-resolution. In *IEEE International Conference on Computer Vision*, pages 1920–1927, 2013.

[39] Zhaowen Wang, Ding Liu, Jianchao Yang, Wei Han, and Thomas Huang. Deep networks for image super-resolution with sparse prior. pages 370–378, 2015.

[40] Fisher Yu and Vladlen Koltun. Multi-scale context aggregation by dilated convolutions. 2016.

[41] Amir R Zamir, Te-Lin Wu, Lin Sun, William B Shen, Bertram E Shi, Jitendra Malik, and Silvio Savarese. Feedback networks. In *Computer Vision and Pattern Recognition (CVPR), 2017 IEEE Conference on*, pages 1808–1817. IEEE, 2017.

[42] Kai Zhang, Wangmeng Zuo, Shuhang Gu, and Lei Zhang. Learning deep cnn denoiser prior for image restoration.

[43] Ting Zhang, Guo Jun Qi, Bin Xiao, and Jingdong Wang. Interleaved group convolutions for deep neural networks. 2017.

[44] Xiangyu Zhang, Xinyu Zhou, Mengxiao Lin, and Jian Sun. Shufflenet: An extremely efficient convolutional neural network for mobile devices. 2017.

[45] Yulun Zhang, Yapeng Tian, Yu Kong, Bineng Zhong, and Yun Fu. Residual dense network for image super-resolution. 2018.